Research Article | Vol. 10, No. 9 / 1 September 2020 / Optical Materials Express 2085
Optical Materials EXPRESS

Novel UV-transparent 2-component polyurethane resin for chip-on-board LED micro lenses

JOACHIM BAUER,[1] MARKO GUTKE,[1] FRIEDHELM HEINRICH,[1] MATTHIAS EDLING,[1] VESELA STOYCHEVA,[1] ALEXANDER KALTENBACH,[2] MARTIN BURKHARDT,[2] MARTIN GRUENEFELD,[3] MATTHIAS GAMP,[3] CHRISTOPH GERHARD,[4] PATRICK STEGLICH,[1,5] SEBASTIAN STEFFEN,[6] MICHAEL HERZOG,[1] CHRISTIAN DREYER,[1,6] AND SIGURD SCHRADER[1]

[1]*Technical University of Applied Sciences Wildau, Hochschulring 1, 15745 Wildau, Germany*
[2]*resintec GmbH, Hellsternstr. 1, 04895 Falkenberg/Elster, Germany*
[3]*EPIGAP Optronic GmbH, Koepenicker Str. 325, Hs. 40, 12555 Berlin, Germany*
[4]*University of Applied Sciences and Arts, Von-Ossietzky-Straße 99, 37085 Göttingen, Germany*
[5]*IHP - Leibniz-Institut für innovative Mikroelektronik, Im Technologiepark 25, 15236 Frankfurt (Oder), Germany*
[6]*Fraunhofer Institute for Applied Polymer Research IAP, PYCO, Kantstr. 55, 14513 Teltow, Germany*
[*]*jobauer@th-wildau.de*

Abstract: In this work we present a novel optical polymer system based on polyurethane elastomer components, which combines excellent UV transparency with high thermal stability, good hardness, high surface tension and long pot life. The material looks very promising for encapsulation and microlensing applications for chip-on-board (CoB) light-emitting diodes (LED). The extinction coefficient k, refractive index n, and bandgap parameters were derived from transmission and reflection measurements in a wavelength range of 200-890 nm. Thermogravimetry and differential scanning calorimetry were used to provide glass transition and degradation temperatures. The surface tension was determined by means of contact angle measurements. As proof of concept, a commercial InGaN-CoB-LED is used to demonstrate the suitability of the new material for the production of microlenses.

1. Introduction

Current requirements and the market volume of light emitting diodes (LEDs) and miniaturized CMOS image sensors have led to an increasing demand for low-cost optics and a notable growth of production capabilities [1–4]. LEDs are regarded as highly efficient light sources that offer a long service life, a wide range of colors and design options. LED chips are generally protected from environmental influences by polymer coatings, where the applied polymer is also used for beam shaping of the emitted light. In addition, the packaging technique should be cost-effective and easy-to-implement. Thus, the optical properties of the polymer coatings are of great importance for the light yield and beam shaping properties.

Conventional optical polymers for encapsulants and lensing of LEDs are epoxy resins [5–8], polymethylmethacrylate (PMMA) [9,10], polycarbonate (PC) [9–12], acrylates [9], polystyrene (PS) [9] and cyclic olefin polymer and copolymer (COP/COC) [9]. Polyurethane (PU) materials are also candidates for the encapsulation of LEDs and organic LEDs (OLEDs) in particular due to their excellent properties for lens formation by evaporative polymer droplet deposition and imprint processes [13,14]. Furthermore, silicone [4,15,16] and silicone hybrid materials, like epoxy–silicone resins [17–20] and sol-gel based siloxane [21–24] are widely used. The

#393844 https://doi.org/10.1364/OME.393844
Journal © 2020 Received 1 Apr 2020; revised 1 Jul 2020; accepted 7 Jul 2020; published 10 Aug 2020

Optical Materials EXPRESS

disadvantages of most conventional polymers are that they are hard and brittle because they have rigid cross-linked networks and decompose under the influence of radiation and high temperature, which leads to chain splitting and discoloration [6–8,10,17]. Silicone resins, on the other hand, have a high thermal stability, UV resistance and are highly transparent in the UV spectral range, but they are relatively soft and have poor adhesion properties [15,16,17]. A further drawback of silicone resins is the refractive index matching of the silicone with respect to the LED material. New material developments to increase lighting efficiency, improve strength and refractive index are achieved by silicone hybrid materials and sol-gel based siloxanes. The combination of materials combines the advantages of conventional polymers such as low cost, easy processing, excellent mechanical properties and good adhesion with the advantages of silicone to improve toughness, internal stresses and thermal stability of encapsulations [17,25]. New research studies have been conducted to improve sealing, insulation resistance, mechanical properties and brightness for conventional optical polymers, silicone and combinations of these materials [25–27]. However, for all materials, except silicone, the transmission is restricted or limited to the visible range.

In this paper, we introduce a novel polymer system that appears promising to overcome this issue. It is based on 2-component polyurethane (PU), which is characterized by easy handling and low manufacturing costs. We show that excellent UV transmission can be achieved with this material. It is well known that aromatic isocyanates are more reactive than aliphatic ones and lead to products with better mechanical properties [28]. Aliphatic isocyanates result in polyurethanes that do not discolor under the influence of light or heat and are highly transparent and thermally stable [29,30]. These media have long pot life, that simplifies the manufacturing process. For LED packaging, the novel material should withstand the soldering processes without impairing the material properties. At the same time, it should meet the requirements of a simple and cost-effective process for the production of a stable encapsulation resin for LEDs with the additional possibility of lens formation. The development of PU according to the above requirements was carried out with the help of various diagnostic methods.

Optical constants in particular play a key role in the selection of suitable optical packaging and lens materials. The targeted application of the novel PU is Chip-on-Board LED micro lens packaging. In this scenario, the refractive index n is essential for (i) refractive index matching with the LED material, (ii) addressing the color dispersion and (iii) optimizing the focal length and the directional characteristics of the polymer micro lenses. The extinction coefficient k is related to absorption and defines the applicability, regarding specific LED emission wavelengths λ. The shortest usable wavelength is defined by the band gap energy E_g, i.e. the transition energy between the highest occupied molecular orbital (HOMO), and the lowest unoccupied molecular orbital (LUMO). For the absorption at photon energies close to the band gap charge trap centers and exciton states play a further role.

Relevant data were derived from optical transmission and reflection (R&T) measurements, using the standard dispersion models Tauc-Lorentz [31,32], Tauc-Lorentz-Urbach [33] and excitonic Lorentz oscillator [34–36]. The extinction coefficients for photon energies well below E_g, particularly relevant for LED packaging and lensing applications, were determined by R&T measurements of thick PU rods and point by point fitting.

Moreover, inhomogeneities within the polymer material must be considered, e.g. differences in density or structural defects, which can lead to local refractive index differences, causing light scattering within the polymer bulk material.

The thermal stability of the LED encapsulation material is an important factor in soldering technology and LED operation. The heat generated in an LED device can lead to outgassing of the material and thus affect the performance of the components in the device. Thermogravimetric analysis (TGA) and differential scanning calorimeter (DSC) were performed to assess the thermal stability of the polyurethanes. The surface tension of polymers and housings are essential for the

Optical Materials EXPRESS

formation of microlenses and determines their radii of curvature. It was derived from contact angle measurements on various substrates based on the harmonic mean approach of Wu [37–39].

2. Experimental

2.1. Materials, synthesis and sample preparation

A group of different PU systems, made by resintec GmbH, was investigated, consisting of the resin-based polyester polyol (PO) with different OH functionalities representing the A-component and different hardeners (B-component), as shown in Table 1. The resins used were resPUR-OT-3000 with a polymeric B-component P-MDI based on methylene diphenyl diisocyanate (MDI), resPUR-OT-T24000 and the material resPUR-OT with an oligomeric B-component O-HDI based on hexamethylene diisocyanate (HDI). The polyurethane (PU) is formed by a polyaddition reaction from the two components by a reaction of the hydroxyl groups (OH) and the isocyanate groups which finally form the urethane groups -NH-CO-O- as part of the repeat unit of the main chain. The A-component is a mixture of polyester polyols with reactive hydroxyl (OH) groups that react with isocyanate (NCO) groups to form the PUs. The number of hydroxyl-(OH)-groups depends on the educts of the polyol synthesis. Aromatic methylenediphenyl diisocyanate polymers and aliphatic isocyanate hexamethylene diisocyanate oligomers are used for the B-components to compare different PUs. The two components were mixed and homogenized with a magnetic stirrer for 2 minutes at a temperature of 50 °C. The specifications of the A- and B-components, the mixing ratios and other material parameters are listed in Table 1.

Table 1. Polyurethane material and component specification.

Polyurethane resPUR	OT-3000	OT-T24000	OT
A-component	PO	PO	PO
Polyol OH content (mgKOH/g)	> 130	> 50	> 130
OH functionality per molecule	2 - 3	2 - 3	2 - 3
B-component	P-MDI	O-HDI	O-HDI
Mixing ratio A/B (weight)	100/44	100/20	100/60
Density at 23 °C (g/mL)	1.17	0.98	1.14
Viscosity at 23 °C (mPa·s)	1,500	19,000	2,000
Shore hardness A at 23 °C	92	64	86
Pot life at 23 °C (min)	30	50	1440
Cure	2 h / 120 °C	1 h / 80 °C	2 h / 120 °C

To determine the absorption coefficients over many orders of magnitude by transmission measurements, samples with different thicknesses were prepared. Thin layers of 5-15 nm thickness were produced by spin coating on quartz substrates. After coating, the material was rapidly thermally annealed at 80 °C for the final curing process. Thick rods of 8 mm width were formed in cuvettes whose walls were removed after curing.

2.2. Thermal investigations

Thermal stability is an important factor in LED encapsulation because the heat generation and heat transfer during soldering can reduce the efficiency of the LED through chemical changes in the polymers. The PUs examined here are generally resistant to high temperatures (10 s at 320 °C and 3 min at 260 °C) and should withstand the soldering process. The degradation temperatures T_d and glass transition temperatures T_g were measured by thermogravimetric analysis (TGA) and differential scanning calorimetry (DSC), using Mettler Toledo TG50 MT5 and Netzsch-DSC-204, respectively.

Optical Materials EXPRESS

2.3. Surface tension measurements

The surface tension or contact angle of the liquid polymer is important for lens formation during dispensing. Contact angles measurements were performed with a commercial system (Surftens from OEG GmbH). The surface tensions of different modified substrates were derived with models of the interaction of molecules according to Wu [37], using the methods given in [38,39]. Using two testing liquids of different polarity it is possible to determine polar σ^p and nonpolar σ^d surface tension of the substrate. In our experiments, water (16-17 MΩcm, $\sigma^p = 50.7$ dyn/cm, $\sigma^d = 22.1$ dyn/cm) and methylene iodide (CH_2I_2, $\sigma^p = 6.7$ dyn/cm, $\sigma^d = 44.1$ dyn/cm) were used. If the surface tension of the substrates is known, the surface tension of liquids can be determined numerically [38,39]. For the determination of the surface tension of polyurethane, different substrates are used, for example silicon with the surface tension of $\sigma^d = 32$ dyn/cm and $\sigma^p = 24$ dyn/cm, glass with $\sigma^d = 35$ dyn/cm and $\sigma^p = 31$ dyn/cm and polytetrafluorethylen (PTFE) modified glass substrate with $\sigma^d = 14$ dyn/cm and $\sigma^p = 2$ dyn/cm.

2.4. Optical analysis

The materials were analyzed in terms of refractive index n and extinction coefficient k in a wavelength range of 200 to 890 nm. For this purpose, optical R&T measurements were performed using different setups and samples with varying thicknesses. The thin-film samples were analyzed in wavelength ranges with strong absorption near and below the bandgap wavelength, whereas the thick rods were used in the low absorption range up to 890 nm. The overall behavior in absorption and transmission was obtained by a commercial spectrophotometer (Lambda 1050, Perkin Elmer) without showing evaluable interference effects due to the relatively low spectral resolution and film thickness inhomogeneities within the illuminated area of about $3 \times 3\ mm^2$. In order to obtain additional information, mainly on the film thicknesses, to be integrated into our fitting model for accurate k and n determination, thin film interferences were evaluated as well. The interference data were obtained by a self-built reflectometer setup (DeepView), described elsewhere [40]. The setup provides a spectral resolution of ~ 0.6 nm in a wavelength range of about 400–600 nm and good interference contrast.

The refractive index n and extinction coefficient k are determined using the two-layer structure model shown in Fig. 1 [41]. The parameters $n(\lambda)$, $k(\lambda)$ and thickness d were determined with the method of least squares from parameterizable models, where experimental and simulated R&T are compared by

$$S(n,k) = \sum_{\lambda_1}^{\lambda_m} \{[R_{sim}(n(\lambda),k(\lambda),d) - R_{exp}(\lambda)]^2 + [T_{sim}(n(\lambda),k(\lambda),d) - T_{exp}(\lambda)]^2\}. \quad (1)$$

The sum $S(n, k)$ executed over the considered wavelength range of λ_1 - λ_m is minimized by a sequential quadratic programming (SQP) algorithm from MATLAB. R_{sim} and T_{sim} are based on incoherent reflection and transmission within the substrate and coherent superposition of the waves within the thin film, which causes the interference effect in the wavelength range of 400 - 600 nm. The simulations concerning spectrophotometer data covering the whole wavelength range were performed incoherently.

The transmission and reflection are calculated according to

$$T_{sim} = \frac{T_0 T_2 T_{sub}}{1 - R_1 R_2 T_{sub}^2} \quad (2)$$

and

$$R_{sim} = \frac{R_0 - R_2 T_{sub}^2 (R_1 R_0 - T_1 T_0)}{1 - R_1 R_2 T_{sub}^2}. \quad (3)$$

All R&T parts R_0, T_0, R_1 and T_1 in Eqs. (2) and (3) were calculated with the help of the matrix method for thin film optics according to Heavens [42]. The parameters n and k are obtained

Optical Materials EXPRESS

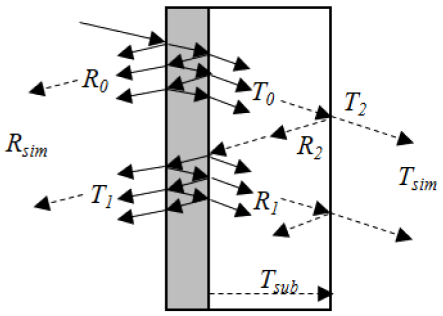

Fig. 1. Schematic representation of the simulation of reflection R_{sim} and transmission T_{sim} considering the multiple incoherent reflections within the substrate and coherent interference effects within the thin film [41]. R_0 is the air side and R_1 the substrate side reflection from the thin film, T_0 is the air to substrate side and T_1 the substrate to air side light transmission through the thin film, R_2 is the substrate/air reflection and T_2 the transmission, respectively, and T_{sub} is the substrate transmission (for quartz $T_{sub} = 1$).

by means of parameterizable models. The optical absorption of polymers can be described by oscillator models generally used in solid-state physics [43]. For polymers the absorption of classical Lorentz oscillators or their extension [43–45] as well as band structure and band gap models [44,46] for π-orbital transitions and / or one-dimensional conjugated or stacked organic materials, based on the Tauc and Davis–Mott model [47–49,53] can be applied. Lorentz models are often used for exciton transitions, which are largely localized in contrast to inorganic semiconductors [50].

Bond orders and polymer backbone kinks and the variations of the lattice configuration influence the electronic structure of polymers close to the band gap. Analogous to inorganic materials, this absorption can be described by the Urbach model [44,51,52].

In this work, we use the Tauc-Lorentz (TL) model [31,32] by including the Urbach tail [33] for the interpretation of transitions from the ground state (e.g. occupied π orbitals of the polymers) to the excited state (e.g. unoccupied π^* orbitals of the polymers) in accordance with the solids.

Based on this oscillator model, the transitions from the highest occupied molecular orbital HOMO to the lowest unoccupied molecular orbital LUMO, i.e. the bandgap E_g, are determined. By transitions from HOMO to LUMO, electron-hole pairs are generated which build excitonic states. In contrast to inorganic semiconductors, the electrons and holes in organic materials are typically localized on the individual molecules and thus form thermally stable Frenkel excitons due to the strong Coulomb interaction [43–45]. In this work, Lorentz distributions given in [34–36] were used for the exciton transitions.

The scattering parameter k_s is determined through R&T measurements by a point by point fit, based on Eq. (1) using simple R&T equations for plane-parallel plates. The fit of k_s is performed in the wavelength range of low absorption ($k \sim 0$).

2.5. Packaging and lens forming

After mixing and homogenizing the two components, the polyurethane microlenses were manufactured on InGaN-CoB-LEDs with chip dimensions of $250 \times 250\ \mu m^2$ in a ceramic package from EPIGAP Optronic GmbH with dimensions of $2 \times 2.5 \times 1\ mm^3$ (width × height × depth) using an Eppendorf EDOS-5221 dispenser. The polyurethane was cured in an oven at 120 °C for 2 hours. Prior to the dispensing, the housing surface was modified with polytetrafluoroethylene (PTFE) to further reduce the radius of the microlens to achieve directed light distribution. The light distributions were measured at a wavelength of 525 nm.

Optical Materials EXPRESS

3. Results and discussion

3.1. Glass and degradation temperature

First stability tests were carried out by exposing the polymers to practical soldering conditions. Optical and mechanical measurements before and after the soldering process showed no changes for the optimized PU resPUR-OT material for a maximum time of 10 s at 320 °C and 3 min at 260 °C. The other two materials did not withstand the soldering process, which was indicated by yellowing after the temperature treatments (see Table 2).

Table 2. Thermal characteristics of polyurethane resPUR.

Thermal Properties		OT-3000	OT-T24000	OT
Glass transition temperature	T_g (°C)	3.0	-42.6	-12.5
DSC-degradation temperature	T_d (°C)	373	356	358
TGA-degradation temperature (5% weight loss)	$T_{d5\%}$ (°C)	349	362	402
Soldering stability test 10 s at 320 °C and 3 min at 260 °C	(°C)	weakly discoloring	weakly discoloring	non discoloring

Figure 2 shows the TGA curves of the PU in the temperature range 30 °C to 600 °C and the 5% weight loss temperature, defined as degradation temperature $T_{d5\%}$. All TGA curves show roughly similar degradation. The DSC curves are presented in Fig. 3 with the glass transition temperatures T_g and degradation temperatures T_d.

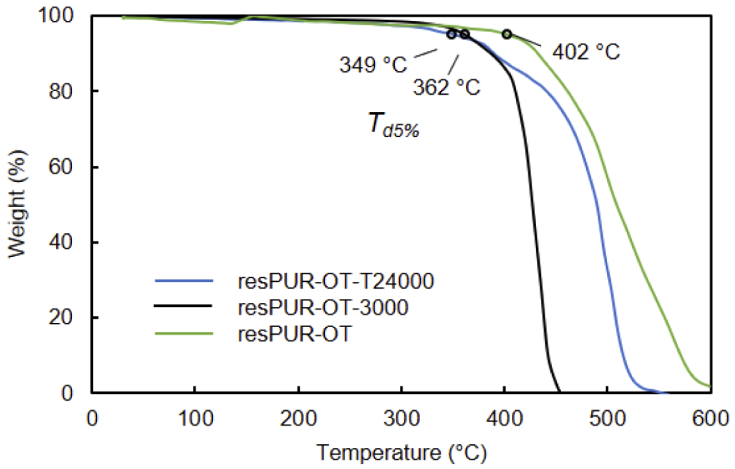

Fig. 2. TGA curve of the Polyurethane, Temperature Program: Heat from 20 °C to 600 °C with a heating rate of 10 °C/min, in Nitrogen atmosphere with a purge rate of 10 mL/minute. The 5% weight loss temperatures $T_{d5\%}$ are marked by circles (o).

According to TGA and DSC analysis, the optimized polyurethane resPUR-OT shows the best properties in terms of thermal stability. With a decomposition temperature > 358 °C the material is well suited for encapsulation purposes.

Optical Materials EXPRESS

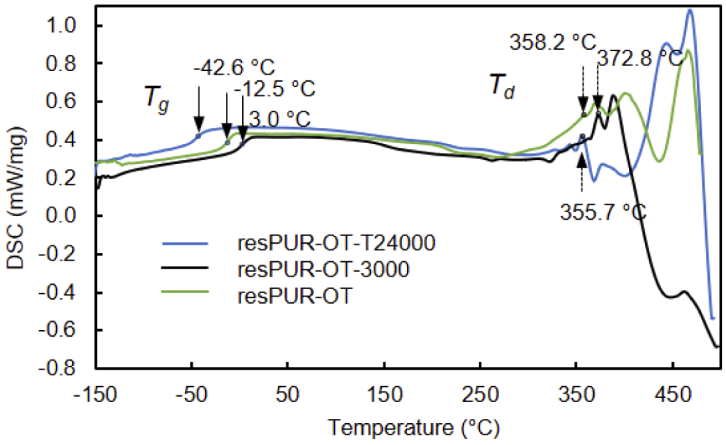

Fig. 3. DSC measurements at temperatures from -150 to 500 °C. The marked points indicate the glass transition temperatures T_g and the degradation temperatures T_d of the polyurethanes. The polymer shows an exothermic reaction at 150 °C for resPUR-OT-3000 and 220 °C for resPUR-OT-T24000 and resPUR-OT polyurethane, probably caused by a crystallization process or postreaction (secondary reaction of isocyanates).

3.2. Surface tension

The microlenses should be produced in a simple and inexpensive dispensing process. Lens formation requires a high surface tension of the material. The surface tension properties are shown in Table 3 and Fig. 4. With a surface tension of 48.4 dynes/cm, the material has excellent droplet formation properties for encapsulation and lens formation. LED chips in ring-shaped or square packages and the modified surface tension of the packages and adapted dosage are determining factors for the radii of curvature of the microlenses, shown in Fig. 4.

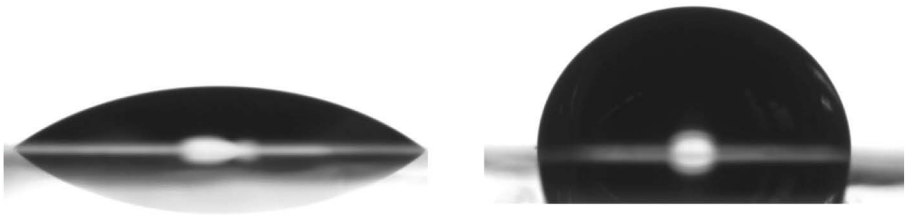

Fig. 4. Contact angles of polyurethane resPUR-OT on different modified substrates: (left) glass with the surface tension of $\sigma^{d} = 35$ dyn/cm and $\sigma^{p} = 31$ dyn/cm and (right) polytetrafluorethylene (PTFE) modified glass substrate with the surface tension of $\sigma^{d} = 14$ dyn/cm and $\sigma^{p} = 2$ dyn/cm, measured by contact angle measurements with water and methylene iodide. Both surfaces are used for the determination of the surface tension of the liquid polyurethane according to [38–40].

Table 3. Surface tension of liquid polyurethanes resPUR.

surface tension	OT-3000	OT-T24000	OT
σ^{d} non polar (dyn/cm)	35.9	34.4	43.7
σ^{d} polar (dyn/cm)	0.4	0.24	4.7

Optical Materials EXPRESS

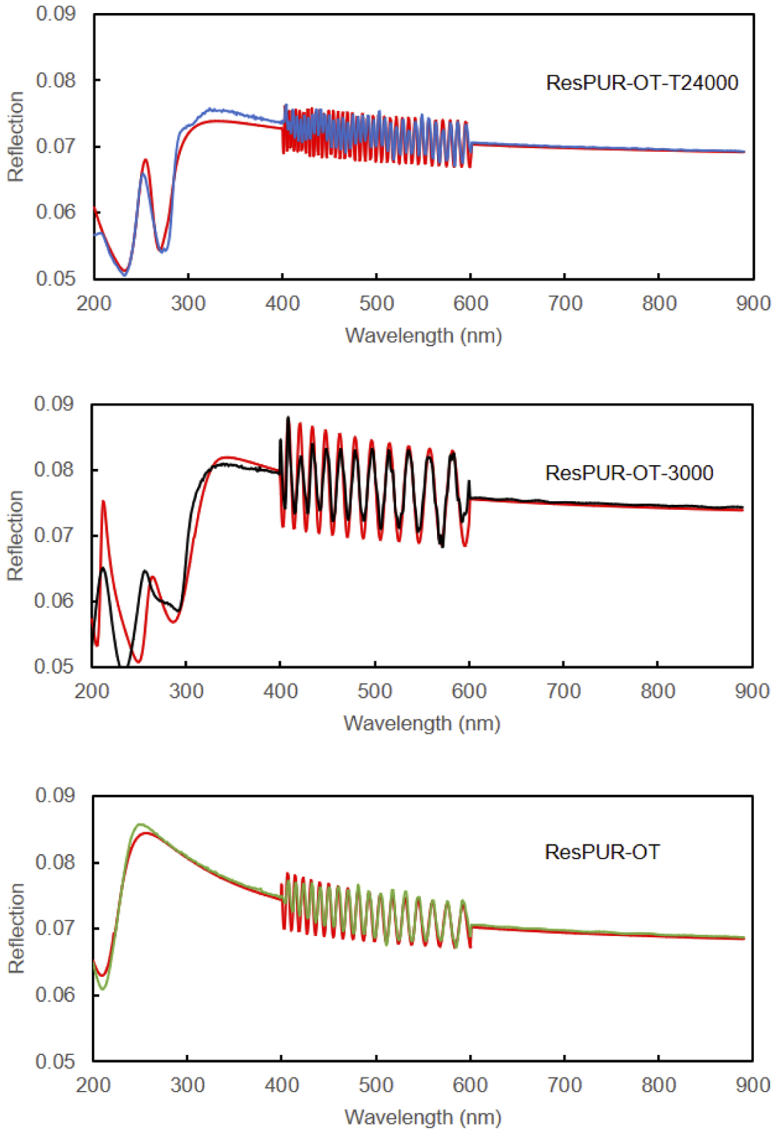

Fig. 5. Experimental and simulated (red) reflection spectra of polyurethane thin films. High-resolution spectra in a wavelength range of 400 - 600 nm were normalized to the low-resolution spectra (200-890 nm) and show typical thin-film interferences, from which the film thicknesses d was determined in the fitting procedure resulting in $d = 13.86$ µm (resPUR OT-T24000), $d = 4.88$ µm (resPUR-OT-3000) and $d = 6.87$ µm (resPUR-OT).

Optical Materials EXPRESS

3.3. Optical properties

Figure 5 and 6 shows R&T spectra of PU thin films. The overall behavior in a wavelength range of 200-890 nm was obtained by the low-resolution spectrophotometer. Superposed and normalized to these data are high spectral resolution reflection measurements providing interferences in a spectral region of 400-600 nm (Fig. 5), used for the thickness determination in our modelling procedure. The corresponding fit curves are marked red. As shown in Fig. 6, the analyzed resin films exhibit quite different transparencies and different band gap energies of 3.89 eV, 4.77 eV and 5.02 eV for resPUR-OT-3000, resPUR-OT-T24000 and resPUR-OT. The transmission attenuation peaks of resPUR-OT-T24000 at a wavelength of $\lambda = 270$ nm and 308 nm in Fig. 6 can be explained by exciton transitions with energies of 4.69 eV and 4.45 eV, whose influence on the dielectric constant reaches far into the 900 nm range (see Fig. 7). This exciton absorption practically prevents the material from being used as encapsulation material for LEDs. The best fit parameter for the resPUR-OT-3000 material leads to two additional interband critical points (CP), which are recognizable by two peaks in the reflection spectrum, as shown in Fig. 5. For resPUR-OT and resPUR-OT-3000 material, the Urbach tail extension was required for parameter setting, which indicates localized states within the band gap. The optical constants n and k determined from the optimized parameters are shown in Fig. 7.

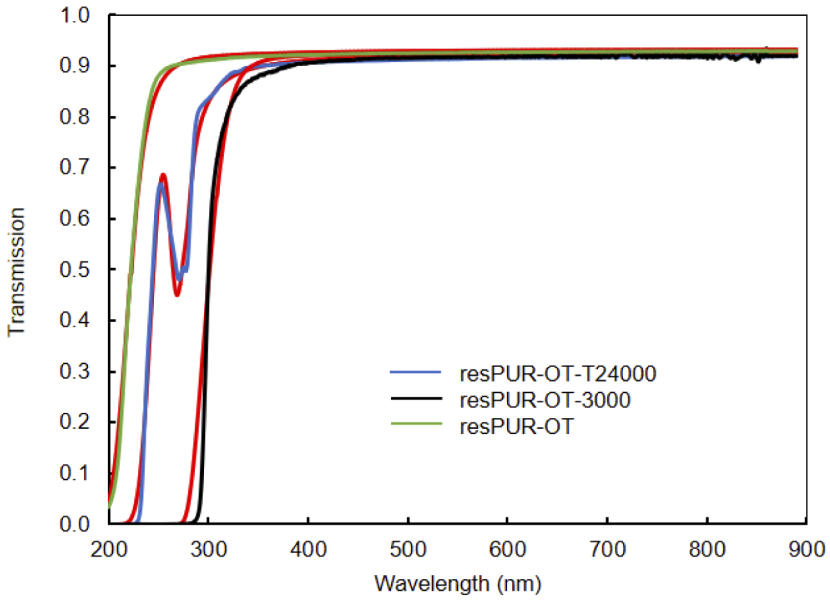

Fig. 6. Experimental and simulated (red) transmission spectra of the PU thin films as shown in Fig. 5 measured with the spectrometer in the spectral range of 200–890 nm. resPUR-OT has the maximum band gap energy of 5,02 eV corresponding to ~ 247 nm.

Scattering was investigated by transmission experiments of the thick PU rods using the spectrophotometer. To quantify the scattering effect, a scattering parameter k_s was defined, so that the effective absorption coefficient is given by $\alpha_e = \alpha + \alpha_s = 4\pi\ (k + k_s)\ /\ \lambda$, where k is the extinction coefficient, α the absorption coefficient and α_s describes the scattering losses. This approach is obvious, since in transmission experiments scattering acts similar to absorption.

The scattering effect could be made visible to the eye with a green laser beam which was guided through the 8 mm thick PU rods. The photos shown in Fig. 8(a) - (c), taken at right angles to the beam axis, show fluorescence as well as strong and weak scattering for the three different polymers, which is in qualitative agreement with the transmission measurements (Fig. 9).

Optical Materials EXPRESS

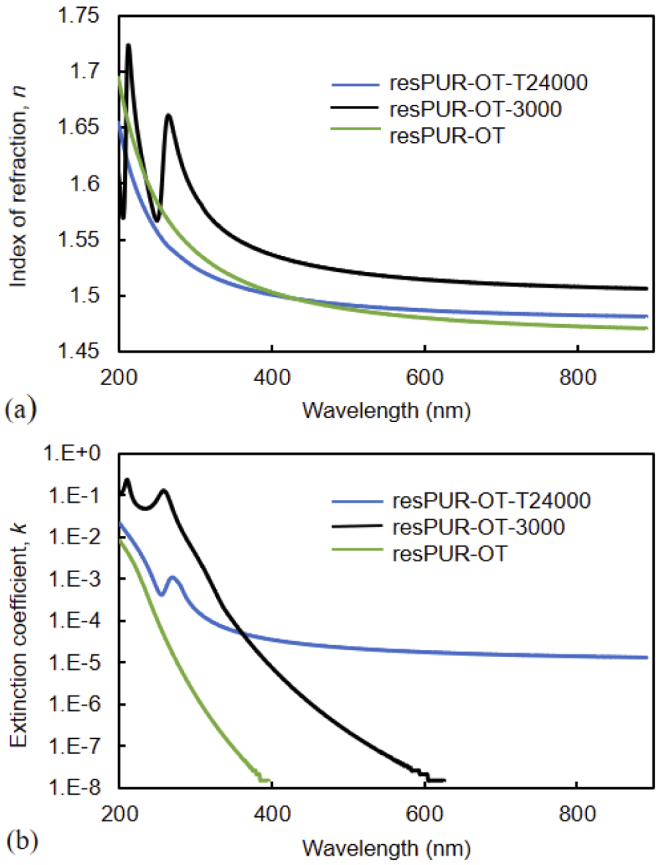

Fig. 7. Optical constants of Polyurethane, (a) refractive index, and (b) extinction coefficient by R&T measurement of thin films and thick PU rods. The relatively high k in the long wavelength region of resPUR-OT-T24000 is caused by the exciton absorption effect.

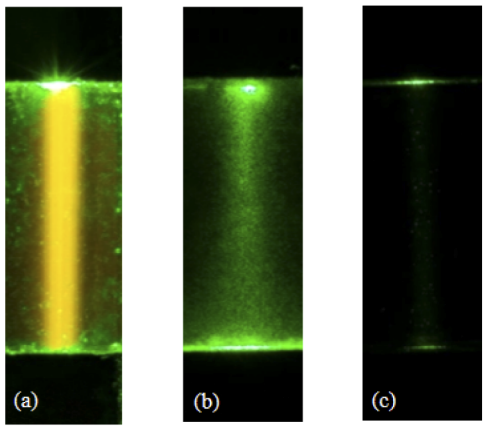

Fig. 8. Frequency doubled 532 nm Nd:YAG laser beam transmitted through the 8 mm thick PU rods of resPUR-OT-3000 (a), resPUR-OT-T24000 (b) and resPUR-OT (c). Photographs taken at right angle to beam direction demonstrate fluorescence (a), strong (b) and weak (c) scattering.

Optical Materials EXPRESS

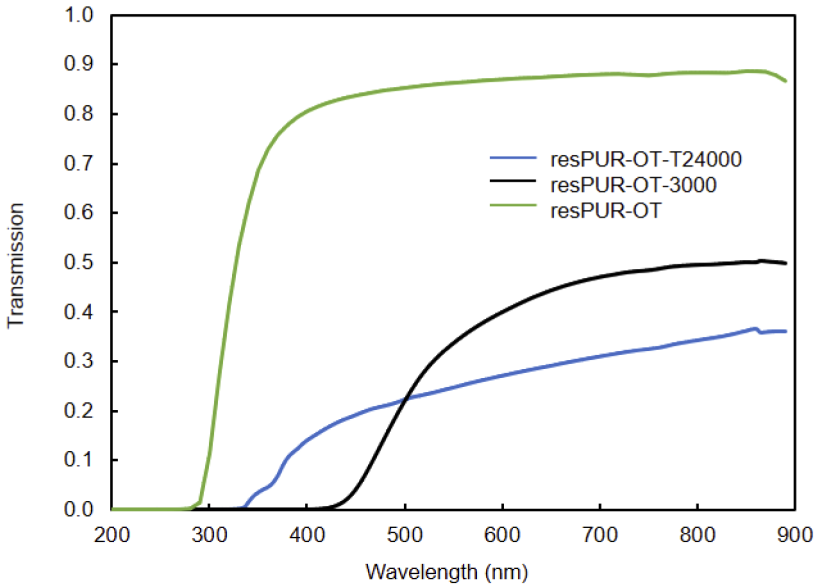

Fig. 9. Experimental transmission spectra of 8 mm thick PU rods. The deviation from the maximum transmission in the long wavelength range can mainly be explained by scattering, which is quite high with resPUR-OT-T24000 and resPUR-OT-3000. In contrast, the optimized material resPUR-OT shows very low scattering.

With this approach, we quantified the scattering part besides the absorbing part. The separation of α and α_s is particularly important in order to estimate the heat transfer to the material which is only determined by α. Especially with high power LED even small α can lead to overheating and degradation of the packaging material, where α_s does not contribute to energy absorption. The scattering parameter k_s, was derived from the fitting procedure, comparing calculated and measured transmission of the PU rods (Fig. 9). The results are shown in Table 4. We have found that k_s depends only weakly on the wavelength and in transmission experiments can be described by Lambert's law in a fairly good approximation. Since $\alpha_s = 4\pi k_s/\lambda$, the corresponding contribution to the effective absorption α_e is wavelength dependent. We assume that scattering is mainly caused by a difference in the refractive indices induced by variations in composition, density differences or structural defects within the polymers. Taking into account the scattering theory of Filinski [53], the application of the Lambert approach leads to changes in the refractive indices in the range from 10^{-4} to 10^{-3}.

In accordance with [29,30], our results show that highly transparent PU can be produced primarily with the B-component HDI. The non-disperse low opacity and fluorescence of resPUR-OT-3000 are caused by the B-component MDI. Furthermore, the conversion of the polyester polyol to a lower OH content compared to the optimized resPUR-OT material leads to the formation of excitons. The optimized polyester with an average OH functionality per molecule of 2 - 3, which corresponds to an OH content expressed by approx. 130 mg KOH/g, was mixed with HDI at a ratio of 100:60. The resulting product (resPUR-OT) was clear, hard-elastic and UV-transparent. The transmission properties of the commonly used optical plastics [9] compared to resPUR-OT are shown in Fig. 10 for a layer thickness of $d = 3.174$ mm. The transmission of PU was calculated using n and k from Fig. 7(a) and (b). With a band gap energy of 5.02 eV the material exhibits excellent transparency in the UV and VIS range and has a moderate Abbe number $\nu_d = (n_d - 1) / (n_F - n_C))$ of 38 (see Table 4). For thin layers, this material can be used up to a wavelength of 300 nm.

Optical Materials EXPRESS

Table 4. Summary of some key characteristics of optical properties of polyurethane resPUR.

Optical Properties		OT-3000	OT-T24000	OT
Refractive index	n_F (486.1 nm)	1.523	1.493	1.49
	n_d (587.6 nm)	1.515	1.488	1.481
	n_C (656.3 nm)	1.512	1.485	1.477
Abbe number	ν_d	47	61	38
Band gap energy	E_g (eV)	3.89	4.77	5.02
Transmission in the visible spectral range, thickness=3.741mm	(%)	0.03-90	67- 82	88-91
Transmission in the UV spectral range (λ=300 nm), thickness=3.741 mm	(%)	0	0	60
Coloring (visual evaluation)		transparent opaque	whitish transparent	clear transparent
Scattering constant	k_s	5.1 E-6	7.5 E-6	3.9 E-7

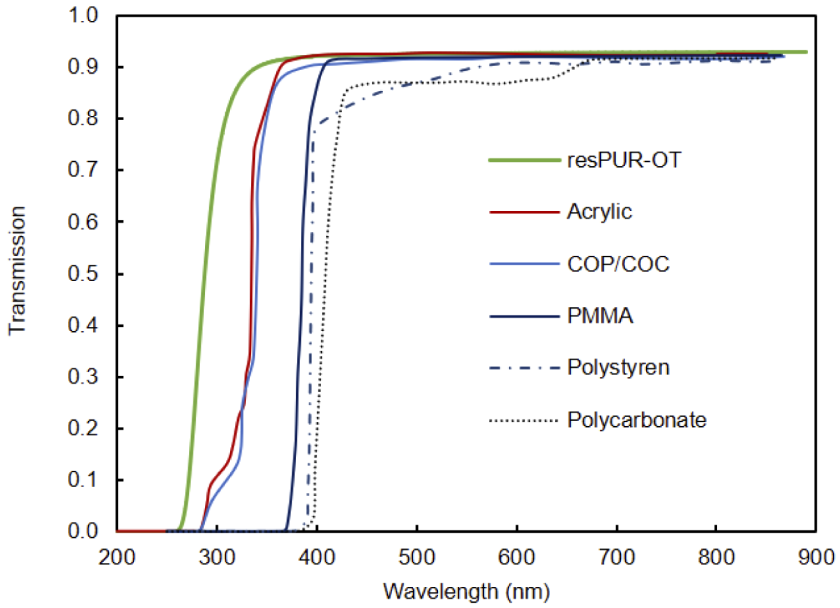

Fig. 10. Transmission of optical polymers [9] compared to polyurethane resPUR-OT at a film thickness of 3.174 mm. The transmission was calculated using the optical constants n and k from Fig. 7(a) and (b).

Optical Materials EXPRESS

3.4. CoB LED lens processing and light distribution

Due to its long pot life, the optimized 2-component polyurethane resPUR-OT proved to be easy to be processed. It showed good lens forming properties, as demonstrated in Fig. 11(a) - (c) on a commercial InGaN-CoB LED in a ceramic package with dimensions $2 \times 2.5 \times 1$ mm^3 (width x height x depth). The size of the diode was 250×250 µm^2. Before dispensing, the outer surface of the ceramic housing was coated with PTFE to reduce the surface tension and thus achieve small lens radii of about 1 mm, as determined from contact angle measurements, described in chapter 2.3. The curing temperatures are given in Table 1.

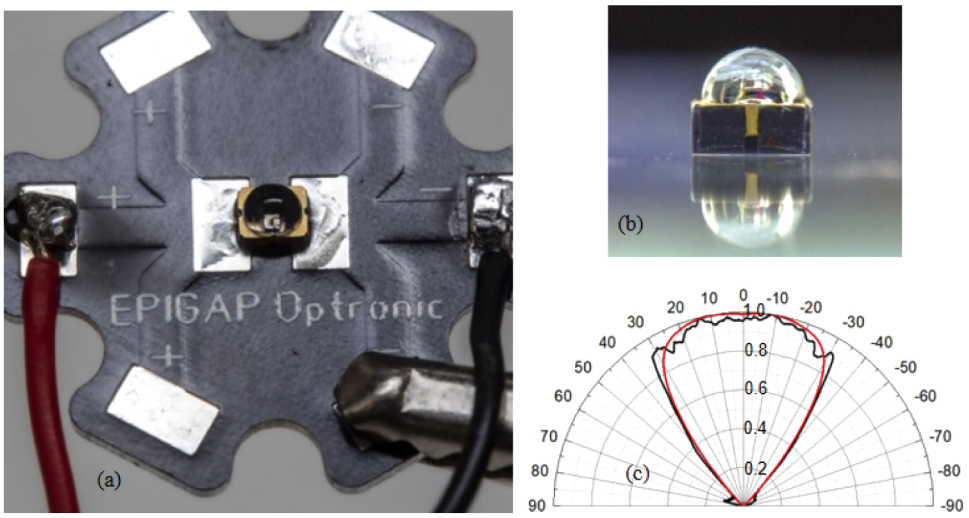

Fig. 11. Dome-Type package of InGaN-CoB-LED with Polyurethane resPUR-OT lens (a), (b) together with measured and simulated (red) light distributions at $\lambda = 525$ nm (c).

Summary

This work confirms that highly transparent polyurethane can be produced from aliphatic isocyanates and polyester polyols by optimizing the mixing ratios. It is demonstrated that the optical properties and the band structure parameter of polyurethanes can be drastically changed by different material components. The method presented here turned out to be a useful approach for the development of optical materials. The optimization of polyurethane elastomer components enables the development of new ingredients and the realization of high-performance optical components. The polyurethane resPUR-OT, developed in this work, has a band gap energy of 5.02 eV and thus excellent transparency in the UV and VIS range. Furthermore, it is characterized by high thermal stability, good hardness and a high surface tension. It offers a simple and cost-effective dispensing technique for the production of micro lenses and enables the manufacture of high-power LEDs with customized beam shaping properties.

Funding

Bundesministerium für Wirtschaft und Energie (16KN074923).

Disclosures

The authors declare that there are no conflicts of interest related to this article.

Optical Materials EXPRESS

References

1. P. Tollay, "Polymer optics gain respect," Photon. Spectra **37**, 76 (2003).
2. K. Angermaier and P. H. Müller, "Zeit und Kosten sparen, UV-härtende Silicone," Carl Hanser Verlag, München, Kunststoffe, 4 (2010).
3. W. M. Lee, A. Upadhya, P. J. Reece, and T. G. Phan, "Fabricating low cost and high performance elastomer lenses using hanging droplets," Biomed. Opt. Express **5**(5), 1626 (2014).
4. C. L. Chang Chien, Y. C. Huang, S. F. Hu, C. M. Chang, M. C. Yip, and W. Fang, "Polymer dispensing and embossing technology for the lens type LED packaging," J. Micromech. Microeng. **23**(6), 065019 (2013).
5. H. Wang, K. S. Lee, J. H. Ryu, C. H. Hong, and Y. H. Cho, "Active packaging method for light-emitting diode lamps with photosensitive epoxy resins," IEEE Photonics Technol. Lett. **20**(2), 87–89 (2008).
6. J. P. Kim, M. S. Jang, W. H. Kim, J. Y. Joo, J. H. Cho, and D. W. Kim, "Improvement in the color uniformity of LED by microspheres generated from phase separation," Opt. Mater. **34**(9), 1614–1617 (2012).
7. N. Gao, W. Q. Liu, Z. L. Yan, and Z. F. Wang, "Synthesis and properties of transparent cycloaliphatic epoxy-silicone resins for optoelectronic devices packaging," Opt. Mater. **35**(3), 567–575 (2013).
8. P. Tao, A. Viswanath, L. S. Schadler, B. C. Benicewicz, and R. W. Siegel, "Preparation and optical properties of indium tin oxide/epoxy nanocomposites with polyglycidyl methacrylate grafted nanoparticles," ACS Appl. Mater. Interfaces **3**(9), 3638–3645 (2011).
9. W. S. Beich and N. Turnera, "Polymer Optics: A manufacturer's perspective on the factors that contribute to successful programs in Polymer Optics Design, Fabrication, and Materials," David H. Krevor and William S. Beich, eds. *Proc. of SPIE* Vol. 7788, 778805 (2010).
10. G. Lu, M. Y. Mehr, W. D. van Driel, X. Fan, J. Fan, and K. M. B. Jansen, "Color Shift Investigations for LED Secondary Optical Designs: Comparison between BPA-PC and PMMA," Opt. Mater. **45**, 37–41 (2015).
11. N. Niessner and D. Wagner, "Practical Guide to Structures, Properties and Applications of Styrenic Polymers," Smithers Rapra Technology (14. März 2013).
12. M. Y. Mehr, W. D. van Driel, K. M. B. Jansen, P. Deeben, M. Boutelje, and G. Q. Zhang, "Photodegradation of bisphenol A polycarbonate under blue light radiation and its effect on optical properties," Opt. Mater. **35**(3), 504–508 (2013).
13. C.-T. Chen, C.-L. Chiu, Z.-F. Tseng, and C.-T. Chuang, "Dynamic evolvement and formation of refractive microlenses self-assembled from evaporative polyurethane droplets," Sens. Actuators, A **147**(2), 369–377 (2008).
14. J.-M. Park, Z. Gan, W. Y. Leung, R. Liu, Z. Ye, K. Constant, J. Shinar, R. Shinar, and K.-M. Ho, "Soft holographic interference lithography microlens for enhanced organic light emitting diode light extraction," Opt. Express **19**(S4), A786 (2011).
15. C. W. Hsu, C. C. M. Ma, C. S. Tan, H. T. Li, and S. C. Huang, "Effect of thermal aging on the optical, dynamic mechanical, and morphological properties of phenylmethylsiloxane-modified epoxy for use as an LED encapsulant," Mater. Chem. Phys. **134**(2-3), 789–796 (2012).
16. W. Huang, Y. Zhang, Y. Z. Yu, and Y. X. Yuan, "Studies on UV-stable silicone–epoxy resins," J. Appl. Polym. Sci. **104**(6), 3954–3959 (2007).
17. K. H. Wu, K. F. Cheng, C. R. Wang, C. C. Yang, and Y. S. Lai, "Study of thermal and optical properties of epoxy/organically modified silicate hybrids," Mater. Express **6**(1), 28–36 (2016).
18. E. Vanlathem, A. W. Norris, M. Bahadur, J. DeGroot, and M. Yoshitake, "Novel silicone materials for LED packaging and optoelectronics devices," Proc. SPIE **6192**, 619202 (2006).
19. Y. H. Lin, J. P. You, Y. C. Lin, N. T. Tran, and F. G. Shi, "Development of high-performance optical silicone for the packaging of high-power LEDs," IEEE Trans. Compon. Packag. Technol. **33**(4), 761–766 (2010).
20. S. C. Yang, J. S. Kim, J. H. Jin, S. Y. Kwak, and B. S. Bae, "Cycloaliphatic epoxy oligosiloxane-derived hybrid materials for a high-refractive index LED encapsulant," J. Appl. Polym. Sci. **122**(4), 2478–2485 (2011).
21. S. Jana, M. A. Lim, I. C. Baek, C. H. Kim, and S. I. Seok, "Nonhydrolytic sol–gel synthesis of epoxysilane-based inorganic–organic hybrid resins," Mater. Chem. Phys. **112**(3), 1008–1014 (2008).
22. S. C. Yang, J. S. Kim, J. H. Jin, S. Y. Kwak, and B. S. Bae, "Thermal resistance of cycloaliphatic epoxy rybrimer based on sol-gel derived oligosiloxane for LED encapsulation," J. Appl. Polym. Sci. **117**(4), 2140–2145 (2010).
23. J. S. Kim, S. C. Yang, and B. S. Bae, "Thermally stable transparent sol-gel based siloxane hybrid material with high refractive index for light emitting diode (LED) encapsulation," Chem. Mater. **22**(11), 3549–3555 (2010).
24. C. L. Chiang, R. C. Chang, and Y. C. Chiu, "Thermal stability and degradation kinetics of novel organic/inorganic epoxy hybrid containing nitrogen/silicon/phosphorus by sol–gel method," Thermochim. Acta **453**(2), 97–104 (2007).
25. C. H. Chen, S. C. Huang, and K. C. Chen, "Novel Siloxane-Modified Epoxy Resins as Promising Encapsulant for LEDs," Polymers **12**(1), 21 (2020).
26. M. Lay, M. R. Ramli, R. Ramli, N. C. Mang, and Z. Ahmad, "Crosslink network and phenyl content on the optical, hardness, and thermal aging of PDMS LED encapsulant," J. Appl. Polym. Sci. **136**(34), 47895 (2019).
27. J. Yang, X. He, H. Wang, X. Liu, P. Lin, S. Yang, and S. Fu, "High-toughness, environment-friendly solid epoxy resins: Preparation, mechanical performance, curing behaviour, and thermal properties," J. Appl. Polym. Sci. **137**(17), 48596 (2020).
28. M. Chanda, "Plastic Technology Handbook," CRC Press Taylor & Francis Group (2018).
29. E. Ayres, W. L. Vasconcelos, and R. L. Oréfice, "Attachment of in organic moieties onto aliphatic polyurethanes," Mat. Res. **10**(2), 119–125 2007.

Optical Materials EXPRESS

30. P. A. Ykman, "Recent Developments in Aliphatic Thermoplastic Polyurethane," ed. in Thermoplastic Elastomer III, palais des congress Brussels, Belgium, April 1991, ISBN 0 902348 52 3.
31. G. E. Jellison and F. A. Modine, "Parameterization of the optical functions of amorphous materials in the interband region," Appl. Phys. Lett. **69**(3), 371–373 (1996).
32. G. E. Jellison and F. A. Modine, "Erratum," Appl. Phys. Lett. **69**(14), 2137 (1996).
33. M. Foldyna, K. Postava, J. Bouchala, J. Pitora, and T. Yamaguchi, "Model dielectric function of amorphous materials including Urbach tail," Proc. SPIE **5445**, 301–305 (2003).
34. M. Cardona, "Modulation Spectroscopy Suppl. vol. 11 to Solid State Physics," F. Seitz, D. Turnbull, and H. Ehrenreich, eds. Academic, New York (1969).
35. P. Lautenschlager, M. Garriga, S. Logothetidis, and M. Cardona, "Interband critical points of GaAs and their temperature dependence," Phys. Rev. B **35**(17), 9174–9189 (1987).
36. D. E. Aspnes, "Modulation spectroscopy/electric field effects on the dielectric function of semiconductors," in *Handbook of Semiconductors*, Vol. 2, M. Balkanski, ed. (North-Holland, 1980) pp. 109–154
37. S. Wu, *Polymer Interface and Adhesion* (Marcel Dekker, 1982).
38. J. Bauer, G. Drescher, and M. Illig, "Surface tension, adhesion and wetting of materials for photolithographic process," J. Vac. Sci. Technol., B: Microelectron. Process. Phenom. **14**(4), 2485 (1996).
39. J. Bauer, G. Drescher, H. Silz, H. Frankenfeld, and M. Illig, "Surface Tension and Adhesion of Photo and Electron-Beam Resists," SPIE Vol. 3049 Advances in Resist Technology and Processing XIV (1997).
40. J. Bauer, O. Fursenko, S. Marschmeyer, F. Heinrich, S. Pulwer, P. Steglich, C. Villringer, A. Mai, and S. Schrader, "Very high aspect ratio through silicon via reflectometry," Proc. SPIE **10329**, 103293J (2017).
41. J. Bauer, "Bestimmung der optischen Konstanten, der Schichtdicke und der Oberflächenrauigkeit dünner Schichten," Experimentelle Technik der Physik **25**(2), 105 (1977).
42. O. S. Heavens, *The Optical Properties of Thin Solid Films* (Butterworth, 1955).
43. A. Köhler and H. Bässler, *Electronic Processes in Organic Semiconductors* (The Electronic Structure of Organic Semiconductors) (Wiley-VCH Verlag GmbH & Co, 2015), 25.
44. A. N. Alias, Z. M. Zabidi, A. M. M. Ali, M. K. Harun, and M. Z. A. Yahya, "Optical Characterization and Properties of Polymeric Materials for Optoelectronic and Photonic Applications," International Journal of Applied Science and Technology **3**, 5 (2013).
45. A. B. Djurisic, T. Fritz, and K. Leo, "Modelling the optical constants of organic thin films: impact of the choice of objective function," J. Opt. A: Pure Appl. Opt. **2**(5), 458–464 (2000).
46. D. K. Seo and R. Hofmann, "Direct and indirect band gap types in one-dimensional conjugated or stacked organic materials," Theor. Chem. Acc. **102**(1-6), 23–32 (1999).
47. N. F. Mott and E. A. Davis, *Electronic Processes in Non-crystalline Materials* (Oxford University Press, 1971).
48. A. N. Alias, Z. M. Zabidi, A. M. M. Ali, M. K. Harun, and M. Z. A. Yahya, "Optical Characterization of Luminescence Polymer Blends Using Tauc/Davis-Mott Model," Adv. Mater. Res. **488-489**, 628–632 (2012).
49. J. Tauc, "Optical Properties of Amorphous Semiconductor," in *Amorphous and Liquid Semiconductor* (Plenum Publishing Company LTD, 1973).
50. W. Brütting and W. Rieß, "Grundlagen der organischen Halbleiter," Physik Journal **7**, 33 (2008).
51. D. A. Tahir, "Optical properties of polymer composite PS-PC thin films," Journal of Kirkuk University –Scientific Studies **5**(2), 87 (2010).
52. A. S. Abed, K. M. Ziadan, and A. Q. Abdullah, "Some optical properties of polyurethane," Iraqi J. of Polymers **17**(1), 18 (2014).
53. I. Filinski, "The effects of sample imperfections on optical spectra," Phys. Status Solidi B **49**(2), 577–588 (1972).